British Journal of Pharmacology (2004) 143, 485–494
www.nature.com/bjp

Selective GABA-receptor actions of amobarbital on thalamic neurons

[1,4,5]H.-S. Kim, [2,5]X. Wan, [3]D.A. Mathers & *,[1,2]E. Puil

[1]Department of Anesthesia, The University of British Columbia, Vancouver, BC, Canada V5Z 4E3;
[2]Department of Pharmacology & Therapeutics, The University of British Columbia, Vancouver, BC, Canada V6T 1Z3 and [3]Department of Physiology, The University of British Columbia, Vancouver, BC, Canada V6T 1Z3

1 We studied amobarbital's effects on membrane properties and currents, and electrically evoked inhibitory postsynaptic currents (IPSCs) mediated by γ-aminobutyric acid (GABA) in rat thalamic slices. Using concentration–response relationships, we compared amobarbital's effects in nociceptive nuclei and non-nociceptive nucleus reticularis thalami (nRT).

2 Amobarbital decreased input resistance by activating $GABA_A$ receptors. Amobarbital produced a larger decrease in ventrobasal than nRT neurons.

3 Amobarbital depressed burst and tonic firing. Depression of burst firing was more effective, particularly in ventrobasal and intralaminar neurons. Depression was reversed by $GABA_A$ antagonists, and surmountable by increasing current injection, implicating a receptor-mediated shunt mechanism.

4 Amobarbital did not affect the tetrodotoxin-isolated low threshold Ca^{2+} spike during $GABA_A$ blockade. Amobarbital reduced excitability without altering outward leak, or hyperpolarisation-activated inward currents.

5 Amobarbital increased mean conductance and burst duration of single $GABA_A$ channels. Consistent with this, amobarbital increased amplitude and decay time of IPSCs with distinct EC_{50}s, implicating actions at two $GABA_A$ receptor sites.

6 Activation of $GABA_A$ receptors by low concentrations, fast IPSC amplitude modulation, and failure to affect intrinsic currents distinguished amobarbital's mechanism of action from previously characterised barbiturates. The selective actions of amobarbital on $GABA_A$ receptor may have relevance in explaining anaesthetic and analgesic uses.
British Journal of Pharmacology (2004) **143,** 485–494. doi:10.1038/sj.bjp.0705974

Keywords: Amobarbitone; barbiturate; GABAergic inhibition; Wada test; anaesthesia; analgesia

Abbreviations: aCSF, artificial cerebrospinal fluid; amo, amobarbital; APV, 2-amino-5-phosphono-valerate; CNQX, 6-cyano-7-nitroquinoxaline; GABA, γ-aminobutyrate; IPSC, inhibitory postsynaptic current; IPSP, inhibitory postsynaptic potential; LTS, low threshold Ca^{2+} spike; nRT, nucleus reticularis thalami; TTX, tetrodotoxin

Introduction

Amobarbital has diagnostic and therapeutic uses, which differ from the general utility of drugs in the barbiturate class. Intracarotid administration of amobarbital induces transient anaesthesia of one cerebral hemisphere, a technique for testing hemispheric competence of memory, cognition, and speech (Wada & Rasmussen, 1960). Amobarbital also produces analgesia in patients with central and neuropathic pain (Mailis *et al*., 1997; Koyama *et al*., 1998). An analgesic property seems paradoxical, in view of the hyperalgesic properties of barbiturates in humans (Hori *et al*., 1984) and *in vivo* preparations (Franklin & Abbott, 1993; but see Cleland *et al*., 1994). Despite extensive studies of barbiturates, the mechanisms responsible for amobarbital's actions remain unclear.

Barbiturates like pentobarbital appear to produce anaesthesia by multiple mechanisms. Pentobarbital depresses neuron excitability in the central nervous system (CNS), interfering with several types of ionic currents (ffrench-Mullen *et al*., 1993; Baudoux *et al*., 2003; Wan *et al*., 2003), in addition to potentiating fast synaptic inhibition mediated by γ-aminobutyrate (GABA; Macdonald & Barker, 1978; Sykes & Thomson, 1989; Krasowski & Harrison, 1999). In thalamocortical neurons *in vitro*, the effects have different concentration–response relationships (Wan & Puil, 2002; Wan *et al*., 2003). These relationships overlap in a concentration range observed upon anaesthetic induction *in vivo*. Despite this apparent redundancy in mechanisms of action, pharmacologists often assume that all barbiturates depress excitability through similar mechanisms. We tested this assumption for amobarbital, which is a chemical isomer of pentobarbital.

The analgesic effects of amobarbital may result from a depression of excitability in neurons that participate in nociceptive transmission at the supraspinal level. Amobarbital relieves pain arising from lesions of the spinothalamic tract

*Author for correspondence at; Department of Pharmacology & Therapeutics, The University of British Columbia, Vancouver, BC, Canada V6T 1Z3; E-mail: puil@neuro.pharmacology.ubc.ca
[4]Current address: Department of Anesthesiology, College of Medicine, Seoul National University, Seoul, Korea.
[5]These authors contributed equally to this work.
Advance online publication: 20 September 2004

(Koyama *et al*., 1998) which provides extensive inputs to thalamus, including ventrobasal nuclei. Neurons in ventrobasal nuclei process somatosensory and viscerosensory information (Krout *et al*., 2002). For example, neurons in human ventrobasal thalamus fire action potential bursts more frequently in central pain conditions (Lenz *et al*., 1989). In this study, we examined the effects of amobarbital on low threshold Ca^{2+} spike (LTS) bursts in neurons of thalamic nuclei that receive different degrees of nociceptive inputs.

We determined amobarbital's effects on the membrane properties, ionic currents, and inhibitory postsynaptic currents (IPSCs) mediated by GABA receptors. Examining their concentration–response relationships, we compared the effects in ventrobasal nuclei and nucleus parafascicularis which receive extensive nociceptive inputs, as well as in non-nociceptive nucleus reticularis thalami (nRT; Yen *et al*., 1989).

Methods

Preparation of thalamic slices

The experiments were approved by the Animal Care Committee of The University of British Columbia. Using previous procedures (Tennigkeit *et al*., 1998; Wan *et al*., 2003), we prepared thalamic slices from brains of Sprague–Dawley rats (13–15 days) under halothane anaesthesia. Horizontal slices (thickness, 300 μm) were cut using a vibroslicer (Campden Instruments, Sileby, U.K.), according to the atlas of Paxinos & Watson (1986). As a guide for positioning the recording electrode, we used sections 100–101 for ventrobasal nuclei, sections 99–100 for intralaminar nucleus, and sections 101–103 for nRT. The slices were incubated for $\geqslant$1 h in oxygenated artificial cerebrospinal fluid (aCSF; 23–25°C) which contained (in mM): 124 NaCl, 26 $NaHCO_3$, 10 D-glucose, 4 KCl, 2 $CaCl_2$, 2 $MgCl_2$, and 1.25 KH_2PO_4. The aCSF solution, saturated with 95% O_2 : 5% CO_2, had a pH = 7.4.

Preparation of dissociated thalamic neurons

We prepared acute dissociated neurons from the slices, described above. Initially, the slices were incubated at 21°C for 10 min in oxygenated, Ca^{2+}-free media of composition (in mM): 120 NaCl, 5 KCl, 1 $MgCl_2$, 5 D-glucose, 20 piperazine-*N*,*N*′-bis(2-ethanesulfonic acid **(**PIPES), 3 ethylene-glycol-bis-(*β*-aminoethyl ether)-*N*,*N*,*N*′,*N*′-tetraacetic-acid (EGTA), and 2 mg ml^{-1} bovine serum albumin (BSA), with pH = 7.3. Prior to incubation, the slices were further blocked with a razor blade to isolate ventrobasal complex or nRT. During incubation, the tissue was stirred for 45 min in a solution of composition (in mM): 120 NaCl, 5 KCl, 1 $MgCl_2$, 1 $CaCl_2$, 20 PIPES, 2 mg ml^{-1} BSA, and 14 U ml^{-1} papain (Sigma Chemical Co., St Louis, U.S.A.) at pH = 7.0 and 32°C. Upon rinsing, the tissue was left for 15 min at room temperature (22°C). We mechanically dispersed the cells in 2 ml Ca^{2+}-free and BSA-free PIPES solution. Upon plating the cells on uncoated 35 mm tissue culture dishes (Corning), the cells remained in PIPES-buffered solution at 21°C until recording.

Whole-cell patch clamp recording

Recording was performed in the whole-cell configuration, in current- and voltage-clamp modes (Wan *et al*., 2003) using an Axoclamp 2A amplifer (Axon Instruments, Union City, U.S.A.). The recording pipettes were forged from 1.5 mm glass tubing with an internal filament (WPI Instruments, Sarasota, U.S.A.). The solution in the recording pipettes contained (in mM): 140 K-gluconate, 5 KCl, 10 *N*-[2-hydroxyethyl] piperazine-*N*′-[2-ethane-sulfonic acid] (HEPES free acid), 10 EGTA, 4 NaCl, 3 $MgCl_2$, 2.8 or 3 adenosine triphosphate disodium salt, and 1 $CaCl_2$, with pH = 7.4 (adjusted with gluconic acid). E_K was −84 mV and E_{Cl} was −53 mV, calculated from the Nernst equation. Electrode resistances varied between 5 and 9 MΩ.

For recording in a Perspex chamber, the slice was perfused at $\geqslant$1 ml min^{-1} with oxygenated (95% O_2 : 5% CO_2) aCSF at 23–25°C. Differential interference contrast microscopy (Zeiss Axioskop, Jena, Germany) was used to visualize cells in nRT, ventrobasal, or intralaminar nuclei. The voltage output of the amplifier was lowpass filtered at 5 kHz and digitised (10 kHz) at 16-bit resolution (pClamp 8 software). A bipolar tungsten electrode (WPI Instruments) was placed in the nRT for evoking IPSCs in ventrobasal or nRT neurons at a holding potential (V_H) in the range of −80 to −30 mV. The electrical stimuli consisted of single pulses (10–90 V, 20–200 μs duration) delivered at 0.5 Hz.

Single channel recording

We recorded single channel currents at ~22°C, as described previously (Wan *et al*., 2003). We utilised dispersed ventrobasal or nRT cells, bathed in a saline containing (in mM): 4 KCl, 135 NaCl, 10 $CaCl_2$, 1 $MgCl_2$, 10 HEPES, and 5 D-glucose, with pH = 7.3. Patch pipettes (10–15 MΩ) were silicone-coated near the tip and contained a solution of composition (in mM): 135 CsCl, 1 $MgCl_2$, 0.267 $CaCl_2$, 10 HEPES, 3 EGTA, and 5 D-glucose, with pH = 7.3. The [Ca^{2+}] was 50 nM. We voltage-clamped outside-out membrane patches usually at V_H = −60 mV (List EPC-7 amplifier). The currents were filtered at DC to 1 kHz, digitised (8 kHz) and analyzed off-line (Instrutech Corp., New York, U.S.A.).

Drugs

GABA, (±)-2-amino-5-phosphonovaleric acid (APV), 1-(3-aminopropyl-)(1′,1′-diethoxy-) methanphosphinic acid (CGP 35348), bicuculline methiodide, 6-cyano-7-nitroquinoxaline-2,3-dione (CNQX), picrotoxinin, and tetrodotoxin (TTX) were purchased from Sigma Chemical Co. Amobarbital (Eli Lilly, Indianapolis, U.S.A.) and other drugs were applied by perfusion of slices or to the external face of outside-out membrane patches.

Data analysis

We subtracted a junction potential of −11 mV from membrane potentials. We used pClamp 8, Prism GraphPad, and CorelDraw software for analysis, including fits of exponential functions to the decay phase of fast IPSCs, averaged from 5 to 10 individual currents. Data were expressed as mean ± s.e.m. and *n* denoted the number of cells. Student's *t*-test was used for

comparing two groups. We used ANOVA for multiple comparisons, and Student–Newman–Keuls tests for comparing group pairs. Significance was defined as $P<0.05$.

The open probability of single channels (P_o) during a period, T_{tot}, was calculated as $P_o=(T_1+2\ T_2+\ldots NT_N)/NT_{tot}$, where N was number of agonist-activated channels and T_1, T_2,.... T_N, were times when at least 1, 2....N channels were open. We transformed open-time distributions by plotting an exponential fit function on logarithmic time scale, yielding a curve with peak amplitude at time constant τ. We calculated the mean open time of agonist-activated channels as the weighted sum of biexponential fits. Distribution of open channel times was fitted by biexponential fits, $y=A_{of}\cdot\exp(-t/\tau_{of})+A_{os}\cdot\exp(-t/\tau_{os})$, where A_{of} = area and τ_{of} = time constant for the fast component, and A_{os} = area, and τ_{os} = time constant for the slow component. We defined groups of openings as bursts, separated by gaps that were briefer than the specified time, t_c. We calculated t_c by solving $1-\exp(-t_c/\tau_{cs})=\exp(-t_c/\tau_{cm})$ for t_c. Here, τ_{cs} and τ_{cm} were slow and medium time constants in the closed time distribution (Colquhoun & Sakmann, 1985). We fitted the closed time distributions for GABA-activated channels with the sum of a triexponential function. This allowed calculation of the mean closed time as a weighted average. We fitted Gaussian terms to amplitude distributions of single channel currents.

Results

Recordings were obtained from 51 ventrobasal, 25 nRT, and five intralaminar neurons that displayed similar values of resting membrane potential and input resistance (R_i). The pooled data showed a mean resting potential of -68 ± 3 mV and mean R_i of 232 ± 17 MΩ ($n=81$).

Amobarbital decreased tonic and burst firing

Amobarbital application (50–500 μM) reversibly decreased tonic firing evoked in all thalamic neurons from near rest. Figure 1a shows this effect upon injection of current pulses into a ventrobasal neuron held at $V_H=-66$ mV. This effect was not dependent on manually clamping the membrane potential to its initial resting value. The suppression of tonic firing was surmountable by injecting larger currents.

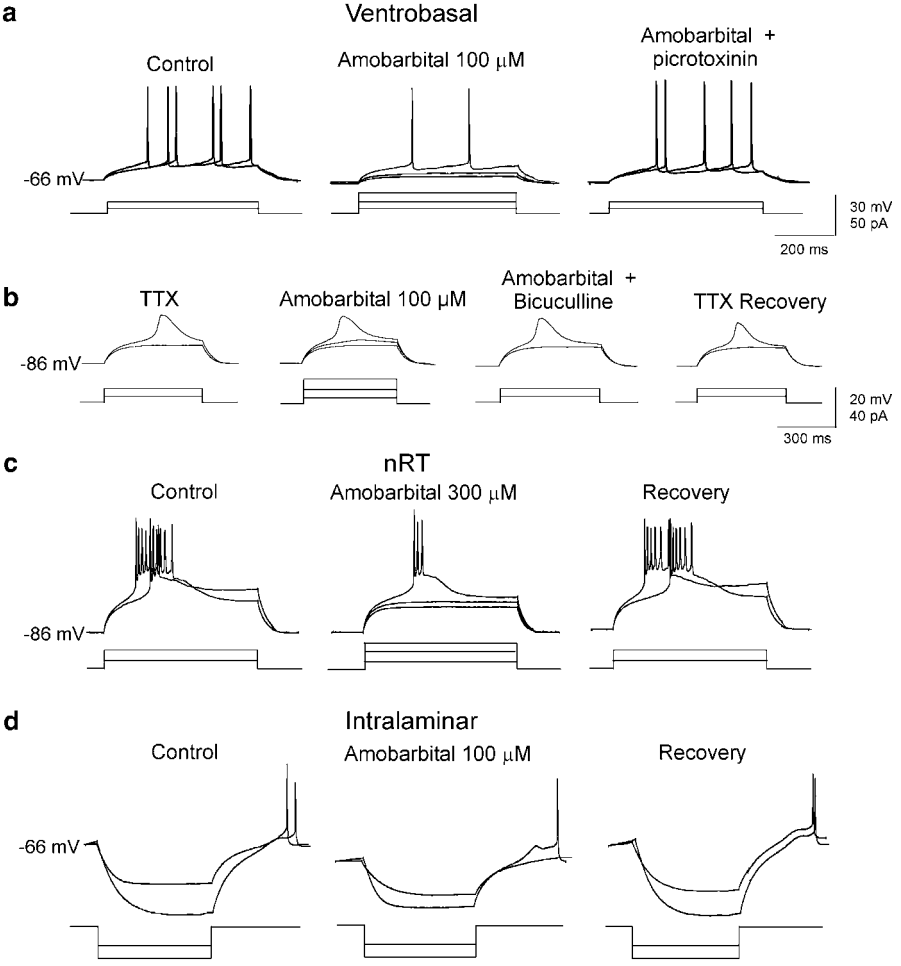

Figure 1 Amobarbital depression of tonic and burst firing in thalamic neurons. (a) Picrotoxinin (50 μM) antagonised the depression of tonic firing in a ventrobasal neuron. (b) Bicuculline blocked amobarbital-induced inhibition of LTS, isolated by application of TTX (0.5 μM) in a ventrobasal neuron. (c) Amobarbital depressed burst firing in nRT neuron, and (d) at offset of hyperpolarising pulse in intralaminar neuron. Lower records in (a–c) show 500 ms current stimuli. Note that larger currents (a–d) or $GABA_A$ blockade (a) partially overcame amobarbital depression. V_H shown at left of voltage records. Calibration in (a) is same as in (c, d).

Amobarbital reversibly decreased LTS bursts in all thalamic neurons. Figure 1c shows this effect upon injection of depolarising pulses into nRT neuron held at $V_H = -86$ mV. Prior to application, action potential discharge associated with the LTS was much less robust in intralaminar neurons. As shown for the intralaminar neuron of Figure 1d, amobarbital application also depressed the LTS and associated firing at the offset of hyperpolarising pulses in all neurons. The suppression of burst firing was surmountable by injecting larger currents (cf. Figure 1c,d).

The decreases in firing were dependent on the amobarbital concentration (Figure 2). The IC_{50} values for the depression of tonic firing were 119 ± 7 μM in ventrobasal, and 99 ± 7 μM in intralaminar neurons. These values were significantly lower than the $IC_{50} = 255 \pm 27$ μM in nRT neurons ($n = 5$, $P < 0.05$). Tonic firing was approximately two-fold more susceptible to amobarbital in ventrobasal and intralaminar neurons than in nRT neurons.

Compared to tonic firing, burst firing was more sensitive to blockade by amobarbital in ventrobasal neurons ($n = 7$; $P < 0.05$) and nRT neurons ($n = 7$; $P < 0.05$). The IC_{50} for the depression of burst firing was 91 ± 7 μM in ventrobasal neurons, substantially lower than the $IC_{50} = 172 \pm 19$ μM in nRT neurons ($n = 5$, $P < 0.05$). Compared to nRT neurons, burst firing in ventrobasal neurons was approximately 80% more susceptible to amobarbital on a concentration basis (Figure 2).

The decrease in burst firing during amobarbital application was partly attributable to a reduced LTS amplitude. We used TTX (0.5 μM) to isolate the LTS from Na^+-dependent action potentials in three ventrobasal neurons. Prior to TTX application, amobarbital reduced the amplitude of the LTS, as estimated near its inflection with the first action potential. As shown for the neuron of Figure 1b, amobarbital (100 μM) still decreased the amplitude of the LTS during its coapplication with TTX. This depression was surmountable with larger currents. Significantly, coapplication of amobarbital with bicuculline (25 μM) in these neurons did not depress the isolated LTS (cf. Figure 1b). Hence, $GABA_A$ receptors likely mediated the amobarbital-induced inhibition of the isolated LTS.

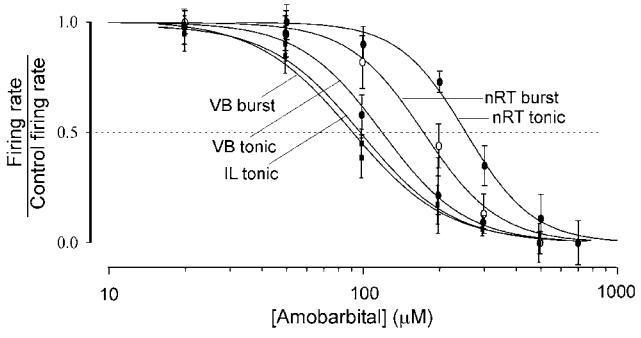

Figure 2 Relationship of concentration to normalised response shows that IC_{50}s for burst suppression were 91 ± 7 μM in ventrobasal (VB burst), and 172 ± 19 μM in nRT (nRT burst) neurons. IC_{50}s for depression of tonic firing were 99 ± 7 μM in intralaminar (IL tonic), 119 ± 7 μM in ventrobasal (VB tonic), and 255 ± 27 μM in nRT (nRT tonic) neurons. Each point represents mean $\pm$ s.e.m. of 3–5 neurons. IC_{50} was lower for depression of burst than for tonic firing in ventrobasal and nRT neurons ($n = 5$, t-test, $P < 0.05$). IC_{50}s for depression of tonic and burst firing were lower in ventrobasal neurons than in nRT neurons ($n = 5$, t-test, $P < 0.05$).

Effects on membrane properties

We examined the hypothesis that the depression of LTS and action potentials resulted from a low resistance shunt. Amobarbital (100 μM) reversibly decreased R_i by 17 ± 6% in ventrobasal neurons (Figure 3a; $n = 5$), and by 18 ± 7% in

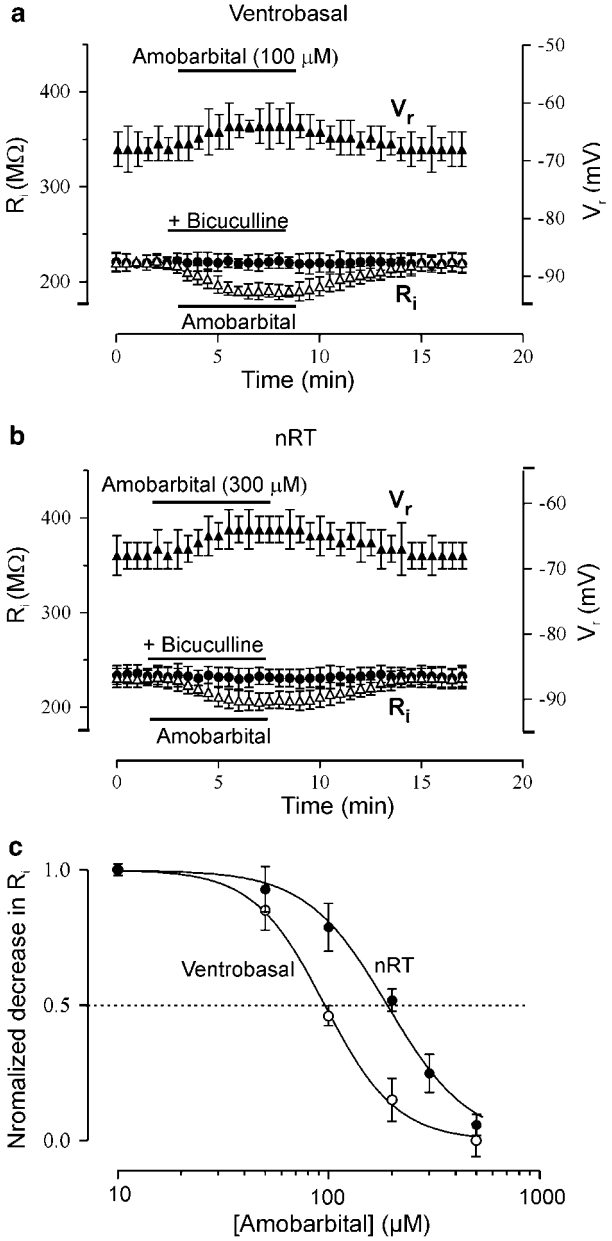

Figure 3 Amobarbital reduced input resistance (R_i) and increased resting membrane potential (V_r) in ventrobasal and nRT neurons. (a, b) Bicuculline (25 μM) antagonised these actions. (c) Concentration–response curves show that amobarbital decreased R_i, with IC_{50}s $= 96 \pm 7$ μM in ventrobasal, and 194 ± 9 μM in nRT neurons, which were significantly different ($n = 5$; t-test; $P < 0.05$). Each data point (mean $\pm$ s.e.m.) represents five neurons in (a) and (b), and 3–5 neurons in (c).

intralaminar neurons ($n=5$). At 100 μM, amobarbital did not significantly change R_i in nRT neurons ($n=5$; $P>0.05$). At 300 μM, amobarbital decreased R_i in nRT neurons by $16\pm4\%$ (Figure 3b). The concentration–response relationships showed that amobarbital decreased R_i with $IC_{50}s=96\pm7$ μM in ventrobasal, and 194 ± 9 μM in nRT neurons (Figure 3c; $n=5$; $P>0.05$).

Amobarbital at 100 and 300 μM produced a depolarisation of 2–5 mV, in association with the changes in R_i. Coapplication with bicuculline (25 μM) or picrotoxinin (50 μM) eliminated the depolarisation and reduction in R_i (cf. Figure 3a, b). Alone, application of bicuculline or picrotoxinin had negligible effects on resting potential and R_i. The effects of amobarbital on membrane potential and R_i implicated $GABA_A$ receptors, and made it unlikely that a leak K^+ current (cf. Wan & Puil, 2002) contributed greatly to its effects on passive membrane properties.

Effects on membrane currents under voltage clamp

As predicted from current-clamp studies, amobarbital application did not significantly affect the leak current (I_{leak}), measured with voltage clamp from the response to a -10 mV hyperpolarising step from -40 mV during blockade of $GABA_A$ receptors with bicuculline (25 μM). I_{leak} in ventrobasal neurons was 25 ± 4 pA before, and 23 ± 5 pA during amobarbital application ($n=5$, $P>0.05$). I_{leak} in nRT neurons was 27 ± 3 pA before, and 28 ± 4 pA during amobarbital application ($n=5$, $P>0.05$).

We determined the effects of amobarbital on voltage-dependent conductances and examined steady-state current–voltage (I–V) relationships in ventrobasal and nRT neurons. Amobarbital increased slope conductance in the range of -40 to -60 mV (Figure 4a, b). Amobarbital induced inward current (I_{Amo}) at potentials negative to -55 mV, which was evident from subtraction of the control current from the current during amobarbital application (right-hand panels, Figure 4a, b). The I_{Amo} curves reversed polarity at -54 ± 3 mV in 24 ventrobasal neurons and -54 ± 2 mV in 12 nRT neurons. These reversals occurred near E_{Cl} (-53 mV), consistent with Cl^- mediation.

Bicuculline or picrotoxinin application abolished the increases in slope conductance induced by amobarbital at 100 μM in ventrobasal neurons, and at 300 μM in nRT neurons. We observed this blockade by picrotoxinin (50 μM) in three ventrobasal (Figure 4a), and three nRT neurons. The application of bicuculline (25 μM) also eliminated the increased slope conductance in three ventrobasal, and three nRT neurons (Figure 4b). No residual current remained upon subtraction of the amobarbital plus $GABA_A$-antagonist curves from the Control curves (right-hand panels, Figure 4a, b).

Nonetheless, our previous studies (Wan *et al*., 2003) showed that pentobarbital decreased I_h, a hyperpolarisation-activated inward current (McCormick & Pape, 1990), which contributed to the nonlinear I–V relationship in a voltage range negative to E_{Cl}. As a further test for amobarbital, we evoked I_h by stepping from $V_H=-50$ to -80 mV, with a pulse of 1 s duration. Maximal amplitude of I_h was not significantly altered in six ventrobasal neurons (control, 53 ± 5 pA and 100 μM amobar-

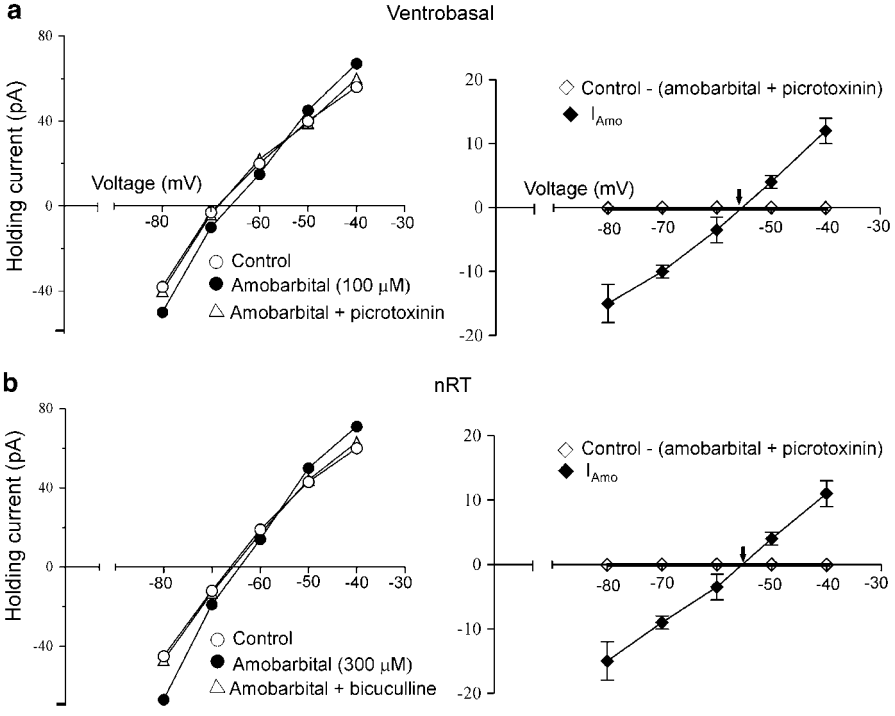

Figure 4 Current–voltage (I–V) relationships for amobarbital actions in two voltage-clamped neurons. (a, b) Amobarbital increased slope of I–V curves which intersected with control curves near -55 mV. Picrotoxinin (50 μM) antagonised amobarbital action on I–V relationships. In right-hand panels of (a) and (b), amobarbital-induced current (I_{Amo}) obtained on subtraction of control from drug curves reversed near -55 mV (arrows). The residual current obtained by subtraction of current during coapplication of amobarbital and picrotoxinin from Control current was near zero pA (right-hand panels of a, b).

bital, 55±6 pA; $P>0.05$) and five nRT neurons (control, 48±5 pA and 300 μM amobarbital, 47±4 pA; $P>0.05$). Hence, amobarbital did not significantly affect I_h in ventrobasal and nRT neurons.

Direct activation of single GABA$_A$ channels

Amobarbital application activated single $GABA_A$ channels. Ventrobasal and nRT membrane patches held at −60 mV exhibited spontaneous, single channel inward currents at a low frequency. Amobarbital (100 μM) greatly increased single channel openings in all patches, as shown for the ventrobasal patch in Figure 5a. Open probability at $V_H=-60$ mV did not differ between ventrobasal and nRT patches.

Amobarbital-activated currents in membrane patches reversed polarity at 0 mV (not shown) which was the same as E_{Cl} in these experiments. Coapplication with bicuculline (50 μM) eliminated the currents in all patches, as shown for the ventrobasal patch of Figure 5a. The reversal of the amobarbital-activated current at E_{Cl} and susceptibility to bicuculline antagonism implicated agonist actions at $GABA_A$ receptors.

Table 1 shows that amobarbital-activated channels exhibited similar conductance behaviour in ventrobasal and nRT patches. The amplitude distributions of amobarbital-activated currents (Figure 5b) showed a prominent peak that corresponded to a conductance state of 23±1.1 pS ($n=5$). In two out of five ventrobasal patches, the channels exhibited a subconductance state of ~16.0 pS (Figure 5a, b). Similarly, the channels in nRT membrane had a full open conductance of 23±1.7 pS ($n=5$), as well as a subconductance state of ~15 pS in two out of five patches.

Amobarbital-activated channels also exhibited similar kinetic behaviour in ventrobasal and nRT patches. Open-time distributions for the channels in ventrobasal and nRT patches were well described by the sum of two exponentials (see Figure 5c). The mean open time did not differ between ventrobasal and nRT patches. For both ventrobasal and nRT patches, scatter plots of current amplitude as a function of open time (cf. Figure 5d) revealed that full open conductance and subconductance states had similar mean open times. Table 1 summarises the observed properties of amobarbital-activated channels in ventrobasal and nRT patches.

Modulation of single channel currents activated by GABA application

We examined the possibility that amobarbital modulated single channel currents during GABA application (10 μM) in ventrobasal and nRT patches. We first identified their susceptibility to bicuculline (50 μM). The GABA-activated

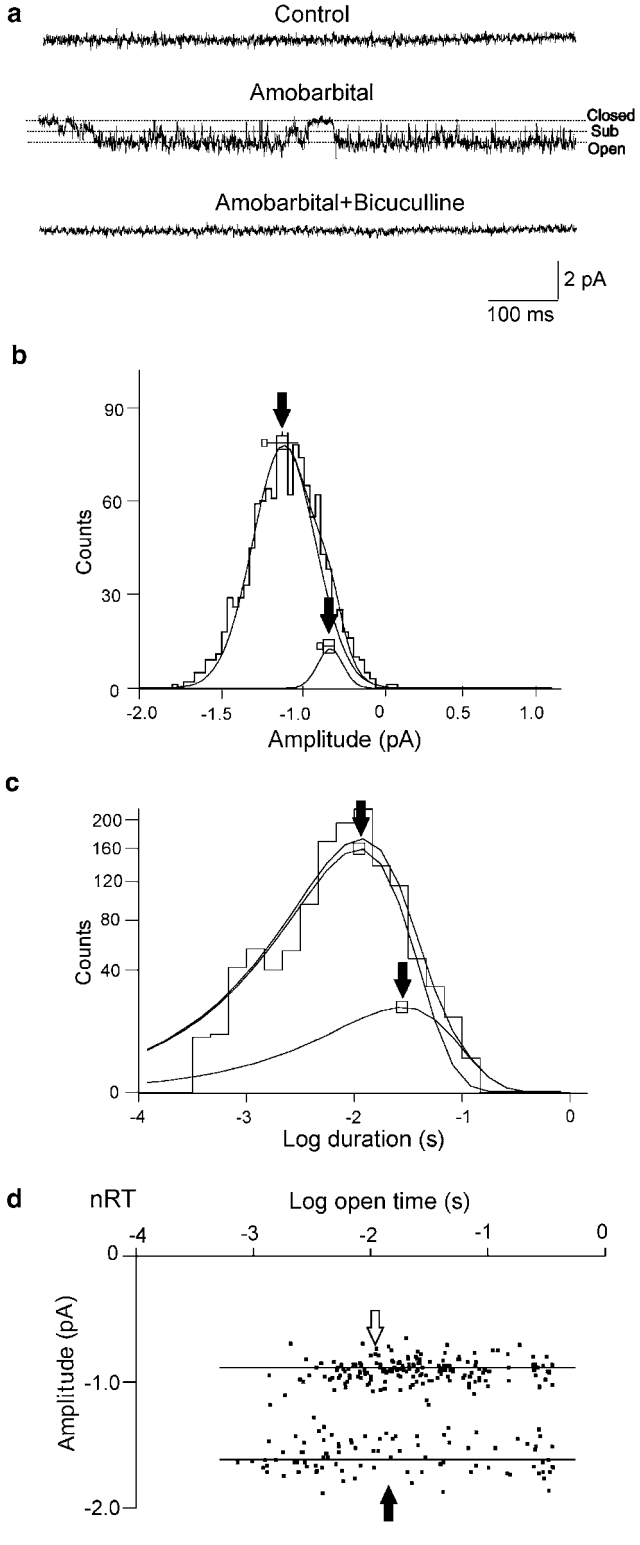

Figure 5 Amobarbital (100 μM) activated single channel currents in ventrobasal (a–c) and nRT (d) patches. (a) Amobarbital induced channel openings with full open state conductance and subconductance (sub) states, blocked by bicuculline (50 μM). (b) Amplitude distribution of activated currents (patch from (a); $n=1239$) was fitted by two Gaussian curves, representing full open (−1.1 pA) and subconductance (−0.7 pA) states (arrows). (c) Distribution of open channel times (patch from a; $n=1234$) was fitted by two exponentials, with $A_{of}=0.89$ and $\tau_{of}=11.1$ ms for fast component, and $A_{os}=0.11$ and $\tau_{os}=28$ ms for slow component. Arrows indicate τ_{of} and τ_{os}. (d) Scatter plot of amplitude as a function of duration for amobarbital-activated currents ($n=526$) shows two discrete populations, with mean amplitudes at −0.9 and −1.6 pA that correspond to subconductance and full open states. The mean open times of 10.9 ms for the substate (open arrow), and 13.1 ms for full open state (filled arrow) were not significantly different. $V_H=-60$ mV.

Table 1 Effects of amobarbital (Amo; 100 μM) on conductance and kinetics of single channel currents activated by GABA (10 μM) or during their co-application

	Ventrobasal membrane patches			*nRT membrane patches*		
	Amo (n = 5)	*GABA* (n = 6)	*GABA + Amo* (n = 6)	*Amo* (n = 5)	*GABA* (n = 7)	*GABA + Amo* (n = 7)
Open probability	0.25 ± 0.06[a]	0.038 ± 0.009	0.39 ± 5.1[bc]	0.31 ± 0.005	0.15 ± 0.038[d]	0.41 ± 0.072[e]
Mean conductance (pS)	20.1 ± 1.4[a]	15.7 ± 0.4	24.1 ± 0.4[bc]	19.2 ± 1.9	16.5 ± 0.8	24.8 ± 2.1[ef]
Mean open time (ms)	14.3 ± 1.1[a]	8.9 ± 0.4	19.2 ± 1.9[c]	16.1 ± 2.4	17.0 ± 2.3[d]	26.7 ± 3.1[def]
Mean closed time (ms)	26.9 ± 13.3[a]	87.8 ± 16.6	22.4 ± 5.9[c]	29.9 ± 10.5	38.2 ± 8.2	28.8 ± 6.2

[a]Significant differences ($P<0.05$) in ventrobasal neurons are denoted as amobarbital *versus* GABA.
[b]Significant differences ($P<0.05$) in ventrobasal neurons are denoted as amobarbital *versus* GABA + amobarbital.
[c]Significant differences ($P<0.05$) in ventrobasal neurons are denoted as GABA *versus* GABA + amobarbital.
[d]Significant differences between neurons are denoted as ventrobasal nuclei *versus* nRT.
[e]In nRT neurons, significance is denoted as GABA *versus* GABA + amobarbital.
[f]In nRT neurons, significance is denoted as amobarbital *versus* GABA + amobarbital.
$V_H = -60$ mV.

currents had an extrapolated reversal potential near 0 mV (not shown), similar to E_{Cl}. These channels had a full open conductance state of ~23 pS in two out of six ventrobasal (cf. Figure 6a), and ~24 pS in two out of seven nRT (cf. Figure 6d) patches. We also observed substate conductance states of 16 ± 0.4 pS in all six ventrobasal, and 17 ± 0.8 pS in all seven nRT patches. The mean conductances of GABA-activated channels were slightly less than observed previously in patches obtained from P8–P13 day rats (Browne *et al*., 2001) and were not significantly different in ventrobasal and nRT patches (Table 1).

Amobarbital (100 μM) coapplied with GABA (10 μM) resulted in currents with amplitude distributions that had a single peak (Figure 6b). The peak corresponded to mean conductances of 24 ± 0.4 pS in ventrobasal, and 25 ± 2.1 pS in nRT patches. The mean conductances were significantly higher than those seen during application of either amobarbital or GABA alone (Table 1). Hence, coapplied amobarbital stabilised the $GABA_A$ receptor in the high conductance state.

Amobarbital modulation of $GABA_A$ receptor channels also was evident in kinetic behaviour in ventrobasal and nRT patches. The mean open probability and open time were significantly increased during coapplication of amobarbital and GABA, compared with GABA alone. Dwell time distributions for ventrobasal channels showed that, compared with GABA alone, the mean closed time was decreased during coapplication of amobarbital and GABA. These data, summarised in Table 1, imply that amobarbital stabilised the $GABA_A$ receptor in open channel configurations.

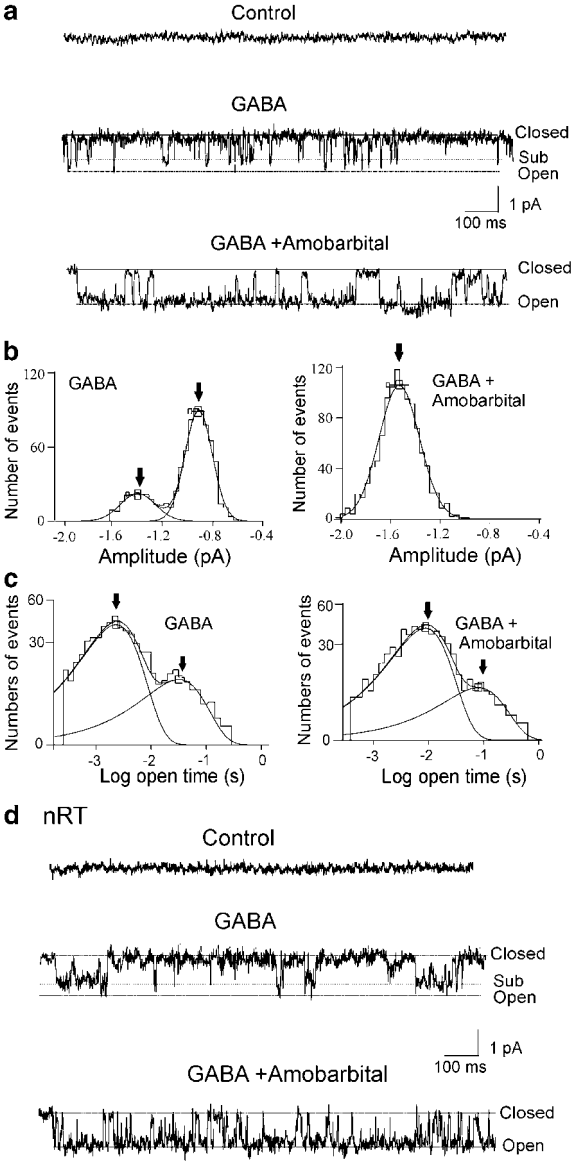

Figure 6 Amobarbital (100 μM) modulated $GABA_A$ channels in ventrobasal (a–c) and nRT (d) patches. (a) GABA (10 μM) induced frequent openings from closed state with full open conductance and subconductance (sub) states. Coapplication of amobarbital with GABA prolonged open time and promoted the full open conductance level. (b, left) Arrows (−1.4 pA and −0.9 pA) in current amplitude histogram during GABA application correspond to full open conductance and subconductance states ($n = 1240$). (b, right) Arrow in current amplitude histogram (−1.5 pA) during coapplication with amobarbital corresponds to full open conductance state ($n = 1476$ events). (c, left) Open-time distribution during GABA application was fitted by biexponential with $\tau_{of} = 2.2$ ms, $A_{of} = 0.8$, $\tau_{os} = 32.0$ ms and $A_{os} = 0.2$ ($n = 798$). (c, right) Open-time distribution during coapplication with amobarbital was fitted with $\tau_{of} = 8.8$ ms, $A_{of} = 0.8$, $\tau_{os} = 80.3$ ms and $A_{os} = 0.18$ ($n = 828$). Arrows in (c; left, right) indicate τ_{of} and τ_{os}. (d) Results similar to (a) were obtained with nRT patch. $V_H = -60$ mV.

Potentiation of amplitude and duration of IPSCs

The single channel results predicted that amobarbital would likely modulate GABAergic IPSCs. We examined amobarbi-

Table 2 Effects of amobarbital (Amo; 100 μM) on fast $GABA_A$ergic IPSCs in ventrobasal and nRT neurons and on burst duration of $GABA_A$ receptor channels

	Ventrobasal neuron or patch		*nRT neuron or patch*	
	Control (n = 5)	*Amo (n = 5)*	*Control (n = 5)*	*Amo (n = 5)*
IPSC amplitude (pA)	42 ± 5	55 ± 6[a]	54 ± 5[b]	67 ± 5[c]
IPSC decay time constant (ms)	20 ± 4	51 ± 7[a]	41 ± 5[b]	64 ± 7[c]
Mean burst duration (ms)	17.8 ± 0.82	46.7 ± 1.7[a]	35.8 ± 1.3[b]	58.3 ± 1.6[c]

[a]Significance ($P<0.05$) in ventrobasal neurons or patches is denoted as Control *versus* amobarbital.
[b]Significant differences between neurons or patches are denoted as ventrobasal nuclei *versus* nRT.
[c]In nRT neurons or patches, significance is denoted as Control *versus* amobarbital.
$V_H = -80$ mV for IPSCs, $V_H = -60$ mV for membrane patches.

tal's effects on the components of IPSCs evoked by electrical stimulation of nRT in 22 ventrobasal and 19 nRT neurons. We evoked IPSCs in all neurons during glutamate receptor blockade with APV (50 μM) and CNQX (25 μM). Miniature IPSCs were not prominent in these recordings. A majority of ventrobasal and nRT neurons exhibited only fast IPSCs, which were entirely susceptible to blockade by 50 μM bicuculline (Figure 7). The fast IPSCs decayed exponentially and reversed polarity at E_{Cl} (not shown). As expected (cf. Huntsman & Huguenard, 2000; Browne *et al*., 2001), ventrobasal IPSCs decayed more rapidly than IPSCs in nRT neurons (Table 2).

Amobarbital (50–500 μM) reversibly increased IPSC amplitude in all ventrobasal and nRT neurons. At 100 μM, amobarbital reversibly increased IPSC amplitude by 31 ± 5% in ventrobasal, and 24 ± 3% in nRT neurons (Figure 7; Table 2). The apparent EC_{50}s for this action were 61 ± 7 μM in ventrobasal (Figure 7a), and 143 ± 18 μM in nRT (Figure 7b) neurons ($P<0.05$).

Amobarbital reversibly prolonged the decay of fast IPSCs in all ventrobasal and nRT neurons (Figure 7). This action was concentration-dependent, with apparent EC_{50}s = 94 ± 11 μM in five ventrobasal, and 309 ± 33 μM in five nRT neurons ($P<0.05$). There was a poor correlation between the decay time constants for fast IPSCs, and the mean open time of GABA-activated channels. However, the decay time constants correlated to mean burst durations of GABA-activated channels, an agreement that persisted during amobarbital application. Prolongation of the fast IPSC was likely due to an amobarbital-induced increase in mean burst duration of $GABA_A$ channels. These data are summarised in Table 2.

Approximately 25% of the IPSCs had a slowly decaying component. This component was apparent in neurons held at E_{Cl} ($E_{Cl} = -53$ mV) and was negligible at $V_H = -80$ mV ($E_K = -84$ mV). Application of a $GABA_B$ receptor antagonist, CGP 35348 (100 nM), abolished the slow component (not shown, $n = 4$). Amobarbital (50–300 μM) did not significantly change the slow component (not shown; $n = 4$, $P > 0.05$), likely due to a $GABA_B$ receptor-gated K^+ conductance (Wan *et al*., 2003).

Table 3 Comparison of EC_{50} and effects of amobarbital and pentobarbital[a]

Thalamocortical neuron parameter	*Amobarbital*	*Pentobarbital*
Blockade of tonic firing (μM)	119 ± 7	7.2 ± 0.7[b]
Increase in IPSC amplitude (μM)	61 ± 7	No effect
Increase in IPSC duration (μM)	94 ± 11	53 ± 4
Decrease in R_i (μM)	96 ± 7	7.8 ± 0.5[b]
Reversal potential (mV)	−54 ± 3	−75 ± 4
T-current underlying LTS	Probably no effect	Probably no effect[b]
I_{leak}	No effect	Increased
I_h	No effect	Decreased
Mean single channel conductance	Increased	No effect
Mean single channel open time	Increased	Increased

[a]Racemate.
[b]Data on pentobarbital from medial geniculate neurons in Wan & Puil, 2002. All other pentobarbital data from ventrobasal neurons in Wan *et al*. (2003).

Discussion

Our principal finding was that $GABA_A$ receptors mediated all observed actions of amobarbital on thalamic neurons. In contrast to other barbiturates, amobarbital was apparently selective in its mechanism of action on thalamic neurons. Direct receptor activation due to amobarbital shunted burst firing more effectively than tonic firing, particularly in neurons that receive nociceptive inputs. Receptor modulation by amobarbital increased the amplitude and decay time of fast IPSCs. The direct activation of $GABA_A$ receptors, amplitude modulation of $GABA_A$ergic IPSCs, a reversal potential for I_{Amo} near E_{Cl}, and failure to affect intrinsic membrane currents unexpectedly distinguished amobarbital from a chemical isomer, pentobarbital (Table 3). These distinctions may relate to the specialised uses of amobarbital in anaesthesia and analgesia.

The most striking effect of amobarbital application was the direct activation of $GABA_A$ receptors. This activation was evident from a decreased R_i, the induction of membrane current (I_{Amo}) that reversed near E_{Cl}, and $GABA_A$ receptor blockade of I_{Amo} and all effects on firing. In single channel studies, amobarbital directly activated Cl^- currents. Bicuculline or picrotoxinin abolished the decrease in R_i, and the macroscopic or single channel currents, induced by amobarbital. On their own, these antagonists had no effect on membrane potential, R_i, or slope conductance. Hence, the effects of amobarbital likely reflected activation of the $GABA_A$ receptor, rather than modulation of endogenous GABA action.

Amobarbital suppressed burst firing more effectively than tonic firing. Both firing modes were more susceptible in ventrobasal and intralaminar neurons than in nRT neurons, not known to receive nociceptive inputs (Yen *et al*., 1989). The suppression was surmountable by stronger depolarising stimuli, and likely due to a decreased R_i. Antagonists of

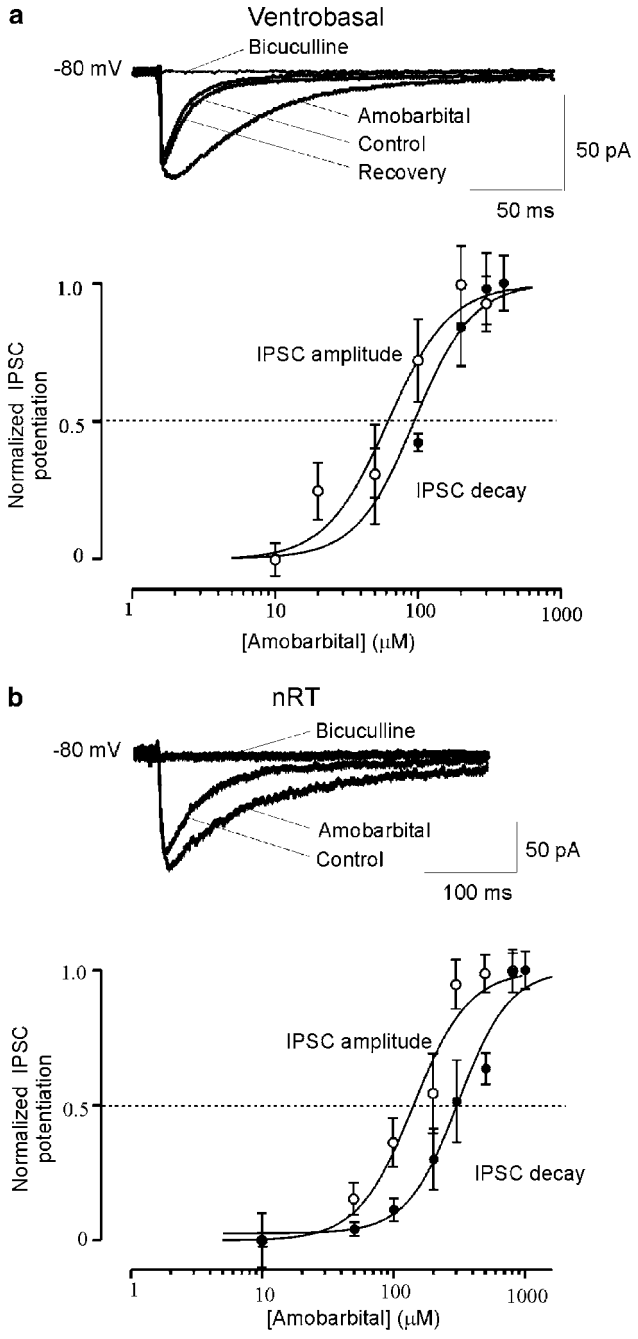

Figure 7 Amobarbital enhanced fast IPSCs in ventrobasal and nRT neurons. (a) Amobarbital (100 μM) reversibly increased amplitude and duration of IPSC. Bicuculline (50 μM) abolished these actions which had apparent EC_{50}s (lower panel) of 61 ± 7 and 94 ± 11 μM. (b) Amobarbital (200 μM) had similar actions on nRT IPSCs, with apparent EC_{50}s (lower panel) of 142 ± 18 and 309 ± 33 μM. Each point represents mean $\pm$ s.e.m. of three to six neurons. $V_H = -80$ mV.

$GABA_A$ receptors abolished this shunt mechanism, and restored the normal firing modes. This effect contrasts with the pentobarbital-induced shunt of firing which persists during complete blockade of GABA receptors (Wan & Puil, 2002; Wan *et al*., 2003).

Amobarbital continued to shunt the LTS during TTX blockade of Na^+-dependent action potentials. The lower IC_{50} for attenuation of LTS bursts may relate to proximal dendritic activation of $GABA_A$ receptors (Pirker *et al*., 2000) which would inactivate T-type Ca^{2+} channels (Ulrich & Huguenard, 1997; Gutierrez *et al*., 2001). Bicuculline completely blocked amobarbital's effects on the TTX-isolated LTS and LTS bursts. Hence, the depression of LTS bursts did not likely result from amobarbital inhibition of Ca^{2+} currents (cf. Gross & Macdonald, 1988; ffrench-Mullen *et al*., 1993), but from the activation of $GABA_A$ receptors.

Amobarbital activated $GABA_A$ receptors with a lower EC_{50} in ventrobasal than in nRT neurons. This is consistent with more abundant α_{1-2} receptor subunits and higher $GABA_A$ channel density in ventrobasal neurons (Wisden *et al*., 1992; Browne *et al*., 2001). Amobarbital increased the open probability of $GABA_A$ channels in both ventrobasal and nRT patches, acting with higher potency than pentobarbital (Wan *et al*., 2003; cf. hippocampal neurons, Rho *et al*., 1996). Direct activation of $GABA_A$ receptors in ventrobasal neurons, which have nociceptive inputs, is consistent with the role of GABA receptors in analgesia (Canavero & Bonicalzi, 1998).

Amobarbital also modulated the actions of endogenous GABA at $GABA_A$ receptors that mediated synaptic inhibition. This modulation increased the amplitude and duration of fast IPSCs, with negligible effects on slow $GABA_B$ IPSCs. Like pentobarbital in hippocampal patches (Birnir *et al*., 2000), amobarbital increased the burst duration of GABA-activated channels, prolonging the fast IPSCs. Single channel analysis showed that amobarbital stabilised the $GABA_A$ receptor in its higher conductance state. Without invoking presynaptic mechanisms (cf. Baudoux *et al*., 2003), this may account for the increased IPSC amplitude in ventrobasal and nRT neurons.

Amobarbital likely had actions at a $GABA_A$ receptor site, additional to that responsible for IPSC amplitude modulation. We infer this from the higher EC_{50}s for potentiating the IPSC duration and activating the $GABA_A$ channel. In contrast, pentobarbital which binds to $GABA_A$ receptor M2 domains (Birnir *et al*., 1997) does not affect IPSC amplitude, yet potently prolongs IPSC duration (Wan *et al*., 2003). Although the use of racemic pentobarbital complicates comparison (cf. ffrench-Mullen *et al*., 1993), amobarbital's extended 5′ side chain conformation may afford a better fit to the amplitude modulation site (cf. Krasowski & Harrison, 1999; Arias *et al*., 2001).

Amobarbital had little or no effect on two intrinsic currents, the leak current (I_{leak}), which we measured during blockade of $GABA_A$ receptors, and I_h. These currents are both susceptible to modulation by pentobarbital (Wan *et al*., 2003). During amobarbital application, a greater IPSP amplitude would enhance I_h. This may promote oscillations or dampen network behaviour (cf. McCormick & Pape, 1990) depending on the Cl^- gradient (Ulrich & Huguenard, 1997), and produce different firing patterns than seen with other barbiturates (cf. Lancel, 1999).

In conclusion, amobarbital had a distinct mechanism of action, summarised in Table 3. Firstly, activation of the $GABA_A$-receptor Cl^- channel complex likely shunted tonic and LTS burst firing. Somatosensory neurons in human thalamus fire action potential bursts more frequently in central pain conditions (Lenz *et al*., 1989). Hence, the preferential depression of burst firing by amobarbital observed in thalamic slices may have clinical importance in central and neuropathic pain (Mailis *et al*., 1997; Koyama *et al*., 1998). Secondly, amobarbital increased mean conductance and burst duration of single $GABA_A$ channels. Such modulation of channels

activated by endogenous GABA likely accounts for the increased amplitude and duration of fast synaptic inhibition. Thirdly, amobarbital reduced neuron excitability without altering I_{leak} or I_h, intrinsic membrane currents. The restricted actions at two sites on the $GABA_A$ receptor may alter firing patterns during anaesthesia and analgesia, in a manner different from other barbiturates.

We are grateful to the Centre for Anesthesia and Analgesia for a Visiting Professorship to Dr Kim and to The University of British Columbia for a University Graduate Fellowship to Dr Wan. We express our gratitude to Viktoriya Dobrovinska for technical support in preparation of slices and dispersed cultures. Amobarbital was a generous gift of Dr Juhn Wada. This study was supported by the Canadian Institutes for Health Research and the Jean Templeton Hugill Chair in Anesthesia held by Dr Puil.

References

ARIAS, H.R., MCCARDY, E.A., GALLAGHER, M.J. & BLANTON, M.P. (2001). Interaction of barbiturate analogs with the Torpedo californica nicotinic acetylcholine receptor ion channel. *Mol. Pharmacol.,* **60,** 497–506.

BAUDOUX, S., EMPSON, R.M. & RICHARDS, C.D. (2003). Pentobarbitone modulates calcium transients in axons and synaptic boutons of hippocampal CA1 neurons. *Br. J. Pharmacol.,* **140,** 971–979.

BIRNIR, B., EGHBALI, M., EVERITT, A.B. & GAGE, P.W. (2000). Bicuculline, pentobarbital and diazepam modulate spontaneous $GABA_A$ channels in rat hippocampal neurons. *Br. J. Pharmacol.,* **131,** 695–704.

BIRNIR, B., TIERNEY, M.L., DALZIEL, J.E., COX, G.B. & GAGE, P.W. (1997). A structural determinant of desensitization and allosteric regulation by pentobarbitone of the $GABA_A$ receptor. *J. Membr. Biol.,* **155,** 157–166.

BROWNE, S.H., KANG, J., AKK, G., CHIANG, L.W., SCHULMAN, H., HUGUENARD, J.R. & PRINCE, D.A. (2001). Kinetic and pharmacological properties of $GABA_A$ receptors in single thalamic neurons and $GABA_A$ subunit expression. *J. Neurophysiol.,* **86,** 2312–2322.

CANAVERO, S. & BONICALZI, V. (1998). The neurochemistry of central pain: evidence from clinical studies, hypothesis and therapeutic implications. *Pain,* **74,** 109–114.

CLELAND, C.E., LIM, F.-Y. & GEBHART, G.F. (1994). Pentobarbital prevents the development of C-fiber-induced hyperalgesia in the rat. *Pain,* **57,** 31–43.

COLQUHOUN, D. & SAKMANN, B. (1985). Fast events in single-channel currents activated by acetylcholine and its analogues at the frog muscle end-plate. *J. Physiol. (London),* **369,** 501–557.

FFRENCH-MULLEN, J.M., BARKER, J.L. & ROGAWSKI, M.A. (1993). Calcium current block by (−)-pentobarbital, phenobarbital, and CHEB but not (+)-pentobarbital in acutely isolated hippocampal CA1 neurons: comparison with effects on GABA-activated Cl− current. *J. Neurosci.,* **13,** 3211–3221.

FRANKLIN, K.B. & ABBOTT, F.V. (1993). Pentobarbital, diazepam, and ethanol abolish the interphase diminution of pain in the formalin test: evidence for pain modulation by $GABA_A$ receptors. *Pharmacol. Biochem. Behav.,* **46,** 661–666.

GROSS, R.A. & MACDONALD, R.L. (1988). Differential actions of pentobarbitone on calcium current components of mouse sensory neurones in culture. *J. Physiol. (London),* **405,** 187–203.

GUTIERREZ, C., COX, C.L., RINZEL, J. & SHERMAN, S.M. (2001). Dynamics of low-threshold spike activation in relay neurons of the cat lateral geniculate nucleus. *J. Neurosci.,* **21,** 1022–1032.

HORI, Y., LEE, K.H., CHUNG, J.M., ENDO, K. & WILLIS, W.D. (1984). The effects of small doses of barbiturate on the activity of primate nociceptive tract cells. *Brain. Res.,* **307,** 9–15.

HUNTSMAN, M.M. & HUGUENARD, J.R. (2000). Nucleus-specific differences in $GABA_A$-receptor-mediated inhibition are enhanced during thalamic development. *J. Neurophysiol.,* **83,** 350–358.

KOYAMA, T., ARAKAWA, Y., SHIBATA, M., MASHIMO, T. & YOSHIYA, I. (1998). Effect of barbiturate on central pain: difference between intravenous administration and oral administration. *Clin. J. Pain.,* **14,** 86–88.

KRASOWSKI, M.D. & HARRISON, N.L. (1999). General anaesthetic actions on ligand-gated ion channels. *Cell. Mol. Life. Sci.,* **55,** 1278–1303.

KROUT, K.E., BELZER, R.E. & LOEWY, A.D. (2002). Brainstem projections to midline and intralaminar thalamic nuclei of the rat. *J. Comp. Neurol.,* **448,** 53–101.

LANCEL, M. (1999). Role of $GABA_A$ receptors in the regulation of sleep: initial sleep responses to peripherally administered modulators and agonists. *Sleep,* **22,** 33–42.

LENZ, F.A., KWAN, H.C., DOSTROVSKY, J.O. & TASKER, R.R. (1989). Characteristics of the bursting pattern of action potentials that occurs in the thalamus of patients with central pain. *Brain. Res.,* **496,** 357–360.

MACDONALD, R.L. & BARKER, J.L. (1978). Different actions of anticonvulsant and anesthetic barbiturates revealed by use of cultured mammalian neurons. *Science,* **200,** 775–777.

MAILIS, A., PLAPLER, P., ASHBY, P., SHOICHET, R. & ROE, S. (1997). Effect of intravenous sodium amytal on cutaneous limb temperatures and sympathetic skin responses in normal subjects and pain patients with and without Complex Regional Pain Syndromes (type I and II). *Pain,* **70,** 59–68.

MCCORMICK, D.A. & PAPE, H.C. (1990). Properties of a hyperpolarisation-activated cation current and its role in rhythmic oscillation in thalamic relay neurones. *J. Physiol.(London),* **431,** 291–318.

PAXINOS, G. & WATSON, C. (1986). *The Rat Brain in Stereotaxic Coordinates,* 2nd edn.. North Ryde: Academic Press.

PIRKER, S., SCHWARZER, C., WIESELTHALER, A., SIEGHART, W. & SPERK, G. (2000). $GABA_A$ receptors: immocytochemical distribution of 13 subunits in the adult rat brain. *Neuroscience,* **101,** 815–850.

RHO, J.M., DONEVAN, S.D. & ROGAWSKI, M.A. (1996). Direct activation of $GABA_A$ receptors by barbiturates in cultured rat hippocampal neurons. *J. Physiol. (London),* **497,** 509–522.

SYKES, T.C.F. & THOMSON, A.M. (1989). Sodium pentobarbitone enhances responses of thalamic relay neurones to GABA in rat brain slices. *Br. J .Pharmacol.,* **97,** 1059–1066.

TENNIGKEIT, F., SCHWARZ, D.W.F. & PUIL, E. (1998). Modulation of bursts and high-threshold calcium spikes in neurons of rat auditory thalamus. *Neuroscience,* **83,** 1063–1073.

ULRICH, D. & HUGUENARD, J.R. (1997). Nucleus-specific chloride homeostasis in rat thalamus. *J. Neurosci.,* **17,** 2348–2354.

WADA, J. & RASMUSSEN, T. (1960). Intracarotid injection of sodium amytal for the lateralization of cerebral speech dominance: experimental and clinical observations. *J. Neurosurg.,* **17,** 266–282.

WAN, X., MATHERS, D.A. & PUIL, E. (2003). Pentobarbital modulates intrinsic and GABA-receptor conductances in thalamocortical inhibition. *Neuroscience,* **121,** 947–958.

WAN, X. & PUIL, E. (2002). Pentobarbital depressant effects are independent of GABA receptors in auditory thalamic neurons. *J. Neurophysiol.,* **88,** 3067–3077.

WISDEN, W., LAURIE, D.J., MONYER, H. & SEEBURG, P.H. (1992). The distribution of 13 $GABA_A$ receptor subunit mRNAs in the rat brain. I. Telencephalon, diencephalon, mesencephalon. *J. Neurosci.,* **12,** 1040–1062.

YEN, C.T., FU, T.C. & CHEN, R.C. (1989). Distribution of thalamic nociceptive neurons activated from the tail of the rat. *Brain Res.,* **498,** 118–122.

(Received May 18, 2004
Revised July 19, 2004
Accepted July 23, 2004)